Journal of Microbiology, Immunology and Infection 56 (2023) 477—489

Available online at www.sciencedirect.com

ScienceDirect

journal homepage: www.e-jmii.com

Original Article

Salmonella typhimurium exacerbates injuries but resolves fibrosis in liver and spleen during *Schistosoma mansoni* infection

Ho Yin Pekkle Lam [a], Wen-Jui Wu [b], Ting-Ruei Liang [c], Hui-Chun Li [a], Kai-Chih Chang [b,d,], Shih-Yi Peng [a,c,*]**

[a] *Department of Biochemistry, School of Medicine, Tzu Chi University, Hualien, Taiwan*
[b] *Department of Laboratory Medicine and Biotechnology, Tzu Chi University, Hualien, Taiwan*
[c] *Ph.D. Program in Pharmacology and Toxicology, School of Medicine, Tzu Chi University, Hualien, Taiwan*
[d] *Department of Laboratory Medicine, Buddhist Tzu Chi General Hospital, Hualien, Taiwan*

Received 1 August 2022; received in revised form 26 January 2023; accepted 7 March 2023
Available online 13 March 2023

KEYWORDS
Schistosomiasis;
Schistosoma mansoni;
Salmonella typhimurium;
Fibrosis

Abstract *Background:* In most developing or undeveloped countries, patients are often co-infected with multiple pathogens rather than a single pathogen. While different pathogens have their impact on morbidity and mortality, co-infection of more than one pathogen usually made the disease outcome different. Many studies reported the co-infection of *Schistosoma* with *Salmonella* in pandemic areas. However, the link or the underlying mechanism in the pathogenesis caused by *Schistosoma-Salmonella* co-infection is still unknown.
Methods: In this study, *Salmonella typhimurium* (*S. typhimurium*) was challenged to *Schistosoma mansoni* (*S. mansoni*)-infected mice. Further experiments such as bacterial culture, histopathological examination, western blotting, and flow cytometry were performed to evaluate the outcomes of the infection. Cytokine responses of the mice were also determined by ELISA and real-time quantitative PCR.
Results: Our results demonstrated that co-infected mice resulted in higher bacterial excretion in the acute phase but higher bacterial colonization in the chronic phase. Lesser egg burden was also observed during chronic schistosomiasis. Infection with *S. typhimurium* during schistosomiasis induces activation of the inflammasome and apoptosis, thereby leading to more

* Corresponding author. Department of Biochemistry, College of Medicine, Tzu Chi University, No. 701, Zhongyang Rd., Sec 3, Hualien 970, Taiwan. Fax: +886 3 857 8387.
** Corresponding author. Department of Laboratory Medicine and Biotechnology, Tzu Chi University, No. 701, Zhongyang Rd., Sec 3, Hualien 970, Taiwan. Fax: +886 3 857 1917.
E-mail addresses: kaichih@mail.tcu.edu.tw (K.-C. Chang), pengsy@mail.tcu.edu.tw (S.-Y. Peng).

https://doi.org/10.1016/j.jmii.2023.03.002

drastic tissue damage. Interestingly, co-infected mice showed a lower fibrotic response in the liver and spleen. Further, co-infection alters the immunological functioning of the mice, possibly the reason for the observed pathological outcomes.
Conclusion: Collectively, our findings here demonstrated that *S. mansoni*-infected mice challenged with *S. typhimurium* altered their immunological responses, thereby leading to different pathological outcomes.

Introduction

Schistosomiasis is a parasitic disease that seriously affects human health worldwide. The major clinical and pathological feature of schistosomiasis is the deposition of eggs in tissues such as the liver and intestine.[1] Once schistosome eggs are trapped in the tissue, they continuously secrete antigenic stimuli that trigger the host's immune response, leading to the formation of granuloma and subsequent fibrosis.[2]

The progression of schistosomiasis can be roughly divided into two stages: acute and chronic stage. Multiple studies showed that during the acute stage, the infected host showed a T-helper 1 (Th1)-dominant response, featuring significant amounts of IFN-γ and IL-2; during the chronic stage, the immune responses shift from Th1 to a robust Th2 response, where IL-4, IL-5, and IL-10 are produced in significant quantities.[2,3] Accordingly, such Th2 immune response has been shown to promote macrophage activation, which facilitated granuloma and fibrosis formation.[4–7]

In most developing or undeveloped countries, patients are often co-infected with multiple pathogens rather than a single pathogen. While different pathogens have their impact on morbidity and mortality, co-infection of more than one pathogen usually made the disease outcome different. For example, patients co-infected with *Schistosoma mansoni* (*S. mansoni*) and *Plasmodium falciparum* worsen the therapeutic outcome and decrease survival rates as these patients have an imbalance of T cells subpopulation and a significantly lower number of memory Treg cells.[8,9] Interestingly, co-infection of *S. mansoni* and *Helicobacter pylori* has been linked with reduced cancer incidence[10] and protection against *S. mansoni*-induced liver fibrosis through immune regulation.[11] These findings implicate that co-infection of more than one pathogen may positively or negatively affect the host's immune response, leading to an altered clinical outcome.

Many studies reported the co-infection of *Schistosoma* with *Salmonella* in pandemic areas.[12–16] Currently, it is known that patients co-infected with *Schistosoma* and *Salmonella* worsen their clinical symptoms.[15,17,18] Animal studies revealed increased bacteriemia, worsened gastrointestinal symptoms, and lower survival in co-infected mice.[19–21] Interestingly, a recent study suggested that *Salmonella typhimurium* infection reduces *Schistosoma japonicum* burden and liver histopathology in mice which may be related to increased IFN-γ and decreased IL-4 levels.[22] While schistosomiasis can be divided into the acute and chronic phases, which induce a very distinct immune response in the host, the link or the underlying mechanism in the pathogenesis caused by *Schistosoma-Salmonella* co-infection is therefore needed for clarification.

Material and methods

Ethics statement

All procedures involving animals were approved by the Institutional Animal Care and Use Committees (IACUC) of Tzu Chi University (No. 110027) and were carried out under approved guidelines of the National Institutes of Health (NIH) Guide for the Care and Use of Laboratory Animals (DHHS publication No. NIH 85—23, revised 1996).

Maintenance of the parasite's life cycle

Puerto Rico strain of *S. mansoni* (*S. mansoni*) was obtained from the Biomedical Research Institute, Rockville, MD 20852, USA, and was maintained in our laboratory.[23] The freshwater snail *Biomphalaria glabrata* was used as an intermediate host and eight-week-old male BABL/c mice (National Laboratory Animal Center, NARLabs, Taipei, Taiwan) were used as the final host. BALB/c mice were housed under a 25 °C $\pm$ 2 °C and a 12 h light/dark cycle condition with free access to water and food.

Bacterial strains and culture conditions

Salmonella typhimurium (*S. typhimurium*) ATCC13311 was purchased from the Bioresource Collection and Research Center (BCRC; Hsinchu, Taiwan). A clinical strain of *S. typhimurium* TCHST1 was obtained from Buddhist Tzu Chi General Hospital (Hualien, Taiwan). Bacteria were streaked from frozen aliquots into Luria Bertani (LB) broth for overnight incubation at 37 °C in a 5% CO_2 incubator. To prepare for infection, bacteria were harvested by centrifugation at 4000$\times g$ for 10 min, washed, and resuspended in sterile water at a concentration of 1×10^8 CFU/mL.

Mice and animal treatment

Eight-week-old male BALB/c mice were used for all experiments. All mice were first subcutaneously infected with 100 $\pm$ 10 *S. mansoni* cercariae. For acute phase experiments, mice were orally gavaged with *S. typhimurium* (1×10^8 CFUs) for three consecutive days four weeks after *S. mansoni* infection. For chronic phase experiments, mice

were orally gavaged with *S. typhimurium* (1×10^8 CFUs) for three consecutive days eight weeks after *S. mansoni* infection. All mice were euthanized one week after the first *S. typhimurium* infection. Upon sacrifice, blood was drawn into heparinized tubes and organs were harvested.

Assessment of bacterial colonization

Weighted fractions of organs were homogenized at 4 °C in sterile phosphate-buffered saline (PBS) using a tissue homogenizer. Bacterial loads were determined by serial tenfold dilutions on Salmonella-Shigella (SS) agar (BD Biosciences, San Jose, CA, USA) incubated at 37 °C for 18 h. Homogenates were then immediately centrifuged at 1500×*g* at 4 °C for 15 min, and supernatants were stored at −80 °C for further assay.

DNA extraction and quantification of bacterial DNA

Bacterial DNA was extracted from weighted stool samples (approximately 200 mg) using the QIAamp® DNA Stool Mini Kit (QIAGEN, Germantown, MD, USA), following the manufacturer's protocol. Real-time quantitative PCR (RT-qPCR) was performed by LabStar SYBR qPCR kit (Bioline, London, UK) using the Roche LightCycler 480 System. RT-qPCR conditions for bacterial detection were 95 °C for 2 min, followed by 40 cycles of 95 °C for 10 s and 55 °C for 10 s. All reactions were finalized with an extension step of 30 s at 72 °C. Total bacterial DNA extracted from *Salmonella typhimurium* ATCC13311 was 10-fold diluted to generate a standard curve. The sequences of the primers used are listed in the S1 Table.

Stool and tissue eggs count

Weighted stool eggs were counted using the Kato-Katz technique.[24] Tissue eggs were counted on weighted tissue fractions after digesting with 4% KOH for 4 h.[25]

Histopathology

Harvested tissues were fixed with 10% formalin, embedded in paraffin, and sectioned into thin slices for hematoxylin & eosin (H&E) and Sirius red staining as previously described.[23] Liver sections were scored for steatosis (both macrovesicular and microvesicular steatosis), inflammation (both lobular and portal inflammation; as presented by foci of polymorphonuclear leukocytes and/or mononuclear cells), necrosis (loss of cytologic details of hepatocyte), and fibrosis (fibrous expansion and/or bridging). Each criterion was assigned a score of 0, absent; 1, mild; 2, moderate; 3, severe.[26] The severity of liver fibrosis was also scored on Sirius red-stained slides according to the Ishak fibrosis scoring system.[27] Spleen sections were scored for the enlargement of lymphocyte areas (increases in the area and number of white pulp elements; 0, absent; 1, mild; 2, moderate; and 3, pronounced) and the presence of apoptosis, necrosis, pigments, and macrophages (each was assigned a score of 0, absent and 1, present).[28] At least ten random fields at 100× magnification were examined and scored in each section.

Hematologic, biochemical, and serological analysis

Complete blood counts (CBC) were determined by a Sysmex KX 21 hematology analyzer (Sysmex Corporation, Taipei, Taiwan) within 2 h of collection. Alanine aminotransferase (ALT), aspartate aminotransferase (AST), and lactate dehydrogenase (LDH) levels from plasma were measured on the Hitachi 7180 chemistry analyzer (Hitachi Ltd., Tokyo, Japan). Concentrations of IL-4, IL-10, IL-2, IL-5, and IFN-γ in the plasma or tissue homogenate were measured using a standard sandwich ELISA kit (Thermo Fisher Scientific, Waltham, MA, USA). Protein concentrations of tissue homogenates were determined by the Bradford method using a Bio-Rad Protein Assay Dye (Bio-Rad Laboratories, Hercules, CA, USA).

Western blotting

Protein samples were separated by sodium dodecyl sulfate-polyacrylamide gels (SDS-PAGE) and transferred onto PVDF membranes (EMD Millipore, Burlington, MA, USA). After blocking with 5% non-fat milk, the membranes were incubated with the following primary antibodies at 4 °C overnight: α-tubulin (GeneTex, Irvine, CA, USA), NLRP3 (Proteintech, Chicago, IL, USA), caspase-1 (Proteintech), IL-1β (Proteintech), IL-18 (Proteintech), caspase-3 (GeneTex), BCL-2 (GeneTex), collagen I (GeneTex), collagen III (GeneTex), and α-SMA (Proteintech). Membranes were then incubated with HRP-conjugated mouse anti-IgG (EMD Millipore) or rabbit anti-IgG (EMD Millipore) secondary antibodies. Membranes were developed using an ECL detection reagent (EMD Millipore). Relative protein levels were quantified using Image J (Version 1.46; National Institute of Health, Bethesda, MD, USA), and protein densitometries were expressed relative to that of α-tubulin.

Flow cytometric analysis

Cell suspension from the mouse liver and spleen was prepared by dispersing the tissue in 8 mL PBS containing 5% fetal bovine serum (FBS; Gibco; Thermo Scientific, Rockford, IL, USA) using a syringe needle. 8 mL red blood cell lysis buffer (0.15 M NH_4Cl, 1 mM $KHCO_3$, 0.1 mM Na_2EDTA; pH 7.2—7.4) were added to lyse the erythrocytes. After centrifugation at 250×*g* for 5 min, cells were resuspended in 5% FBS-containing PBS and were passed through a 70 μm nylon mesh cell strainer (Corning, Inc., Corning, NY, USA).[23] The cells were then stained by Alexa Fluor Annexin V/Dead Cell Apoptosis kit (Molecular Probes Inc., Eugene, OR, USA) according to the manufacturer's instruction and analyzed using a Gallios™ 10-channel flow cytometer (Beckman Coulter, Brea, CA, USA).

Real-time quantitative polymerase chain reaction (RT-qPCR)

Total RNA was isolated from tissues using TRIzol reagent (Thermo Scientific) according to the manufacturer's instructions. Five micrograms of total RNA were used for cDNA synthesis using a RevertAid first-strand cDNA synthesis kit (Fermentas International Inc., Burlington, ON, Canada).

RT-qPCR was performed with the LabStar SYBR qPCR kit (Bioline) using the Roche LightCycler 480 System. The primers used in this study are shown in Supplementary Table 1. Relative gene expression was calculated using the $2^{-\Delta\Delta CT}$ method and gene expression levels were normalized to *β-actin*.

Immunohistochemistry staining

Paraffin slides were deparaffinized and rehydrated. Antigens were retrieved from the sections by soaking them in boiling EDTA buffer for 20 min. Subsequently, the sections were blocked with 3% H_2O_2 for 10 min and 10% FBS for 1 h. Thereafter, the sections were incubated overnight at 4 °C with the following primary antibodies: CD68 (ABclonal), CD4 (ABclonal), and CD8 (ABclonal). The sections were then incubated with HRP-conjugated secondary antibody (EMD Millipore) for 30 min and 3,3′-diaminobenzidine (DAB; Thermo Scientific) for 3 min. Sections were counterstained with Hematoxylin and rehydrated with increasing concentrations of ethanol prior to mounting.

Statistical analysis

All experimental data were analyzed using GraphPad Prism 6.01 software (GraphPad Software Inc., San Diego, CA, USA). Unless stated otherwise, data are represented as the mean ± standard error mean. To compare two groups, the Mann—Whitney U test was used; to compare more than two groups, a one-way analysis of variance (ANOVA) was used with Tukey's post-hoc test to estimate statistical differences between groups. Significant differences were taken into consideration with a p-value < 0.05.

Results

Chronic schistosomiasis increases *S. typhimurium* colonization but decreases eggs deposition in tissues

To explore the effect *S. typhimurium* had on different stages of *S. mansoni* infection, *S. typhimurium* was infected in *S. mansoni*-infected mice when it reaches the acute phase (4-week post-*S. mansoni* infection) or chronic phase (8-week post-*S. mansoni* infection). Since previous studies found that mice co-infected with *S. mansoni* and *Salmonella* had higher bacterial colonization and resulted in a higher mortality rate,[20,21] we first investigated bacterial colonization, as well as egg deposition in different tissues. It was found that during the acute phase, co-infected mice had higher *S. typhimurium* copies in stool, and this was accompanied by a slight decrease of *S. typhimurium* colonization in the liver and spleen (Fig. 1A and B; Supplementary Fig. 1A and B). During the chronic phase, co-infected mice had significantly lower *S. typhimurium* copies in stool, and higher *S. typhimurium* colonization in the liver and spleen (Fig. 1D and E; Supplementary Fig. 1D and E). At the same time, schistosome eggs were detected in neither stool nor livers during the acute phase (Fig. 1C; Supplementary Fig. 1C); where a decrease of schistosome eggs was detected in livers of co-infected mice, compared

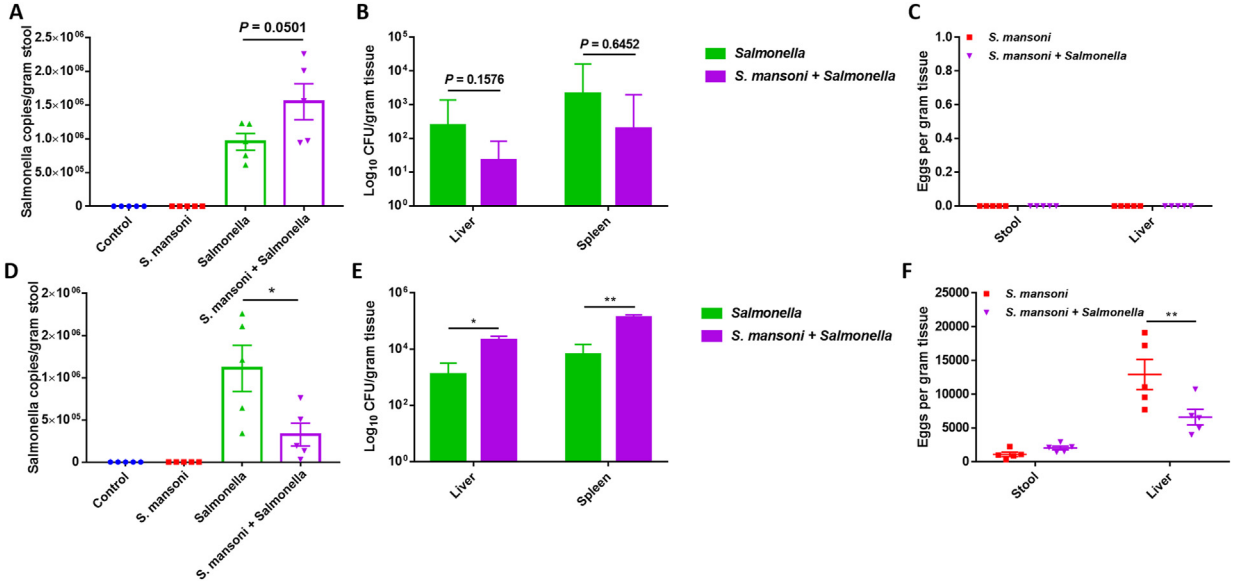

Figure 1. Higher *S. typhimurium* colonization and lower egg deposition during chronic phase of *S. mansoni* infection. (A) A higher number of *S. typhimurium* was recovered from stool in co-infected mice during acute schistosomiasis. (B) A slightly lower number of *S. typhimurium* was recovered from livers and spleens in co-infected mice during acute schistosomiasis. (C) No *S. mansoni* eggs were found from stool or livers during acute schistosomiasis. (D) Lower number of *S. typhimurium* was recovered from stool in co-infected mice during chronic schistosomiasis. (E) Higher *S. typhimurium* was found in the liver and spleen of co-infected mice during chronic schistosomiasis. (F) Lower number of *S. mansoni* eggs was recovered from stool or tissues of co-infected mice during chronic schistosomiasis. All *S. typhimurium* strains used here were TCHST1. Data are shown as mean ± standard error mean (n = 5 per group). *$p < 0.05$ and **$p < 0.01$.

to mice infected only with *S. mansoni* (Fig. 1F; Supplementary Fig. 1F). These results indicate that *S. typhimurium* infection during acute schistosomiasis decreases their colonization of tissues and increases their stool excretion; whereas coinfection at the chronic phase retained bacteria in the tissues which corroborates a previous study[21] and may lower eggs entrapment in tissues or, somehow, decrease the worm's reproduction activities.

S. typhimurium worsens liver injuries during chronic schistosomiasis

Next, we investigated whether *S. typhimurium* co-infection worsens *S. mansoni*-induced symptoms. Results were as expected as *Salmonella* is not retained in the liver during acute schistosomiasis, and liver injuries were similar in co-infected mice compared with *S. mansoni*-infected mice (Fig. 2A–C, G, I, and K; Supplementary Fig. 2A–C, G, I, and K). However, in the chronic phase, co-infected mice showed higher histological pathology and liver function markers (Fig. 2D–F, H, J, and L; Supplementary Fig. 2D–F, H, J, and L), suggesting that the colonized *S. typhimurium* worsened *S. mansoni*-induced liver injuries in the chronic phase. To this end, we analyzed several injury-related markers that were shown to increase in the liver during schistosomiasis including inflammasome and apoptotic proteins.[23] We confirmed that during the acute phase NLRP3 inflammasome components, as well as apoptotic markers, were of similar expression in co-infected mice, compared with *S. mansoni*-infected mice. *S. typhimurium* mono-infection, except for the increased caspase-3 expression, also gives similar protein expression to other markers with *S. mansoni*-infected mice (Fig. 3A and B; Supplementary Fig. 3A). Flow cytometric analysis confirmed that *S. typhimurium* infection in *S. mansoni*-infected mice did not affect the existing apoptosis in livers (Fig. 3C). On the other hand, co-infected mice at the chronic phase significantly increased liver expression of inflammasome and apoptotic proteins (Fig. 3D and E; Supplementary Fig. 3B) and resulted in significantly higher apoptotic cells (Fig. 3F) compared with the mono-infected group. These data corroborate with the histology findings, suggesting that the liver-colonized *S. typhimurium* significantly worsens the symptoms of chronic schistosomiasis.

S. typhimurium decreases collagen deposition and liver fibrosis during chronic schistosomiasis

We further determined whether *S. typhimurium* infection would exacerbate liver fibrosis of *S. mansoni*-infected mice. *S. typhimurium* infection at the acute phase only slightly but not statistically significantly aggravated liver fibrosis in *S. mansoni*-infected mice (Fig. 4A, C, and E;

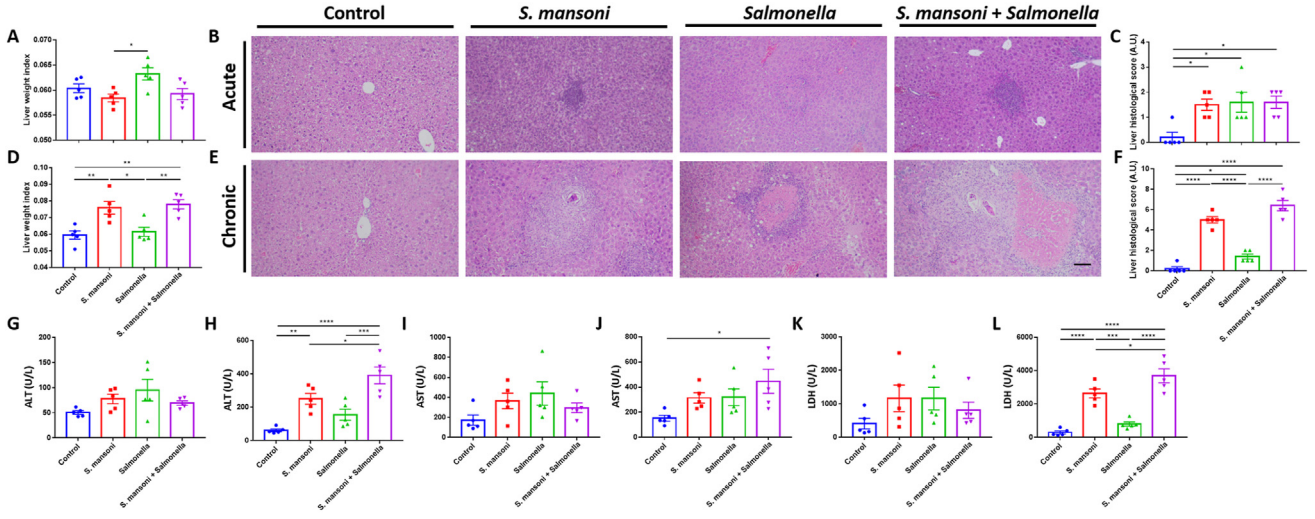

Figure 2. ***S. typhimurium* worsens liver injuries during chronic schistosomiasis but not acute schistosomiasis.** (A) Weight index of the liver (liver weight/body weight) of mice during the acute phase. (B) Representative H&E-stained histological image of the liver during the acute phase. Liver from *S. mansoni*-infected mice and co-infected mice showed cellular infiltration whereas liver from *S. typhimurium*-infected mice showed congestion and necrosis. (C) Histological scores of livers during the acute phase. (D) Liver weight index during the chronic phase. (E) Representative histological image of the liver during the chronic phase. Liver from *S. mansoni*-infected mice showed schistosome eggs surrounded by granuloma and infiltration whereas *S. typhimurium*-infected mice showed congestion and necrosis. Co-infected mice showed both pathological findings but to a greater extent. Images are shown as 100× magnification and scale bars correspond to 200 μm. (F) Histological scores of livers during the chronic phase. (G–L) Serum alanine transaminase (ALT) level during (G) acute phase and (H) chronic phase; aspartate transaminase (AST) level during (I) acute phase and (J) chronic phase; lactate dehydrogenase (LDH) level during (K) acute phase and (L) chronic phase. These serum markers were significantly elevated in co-infected mice during chronic schistosomiasis, compared with mice with *S. mansoni* infection only. All *S. typhimurium* strains used here were TCHST1. Data are shown as mean ± standard error mean (n = 5 per group). *$p < 0.05$; **$p < 0.01$, ***$p < 0.001$, and ****$p < 0.0001$.

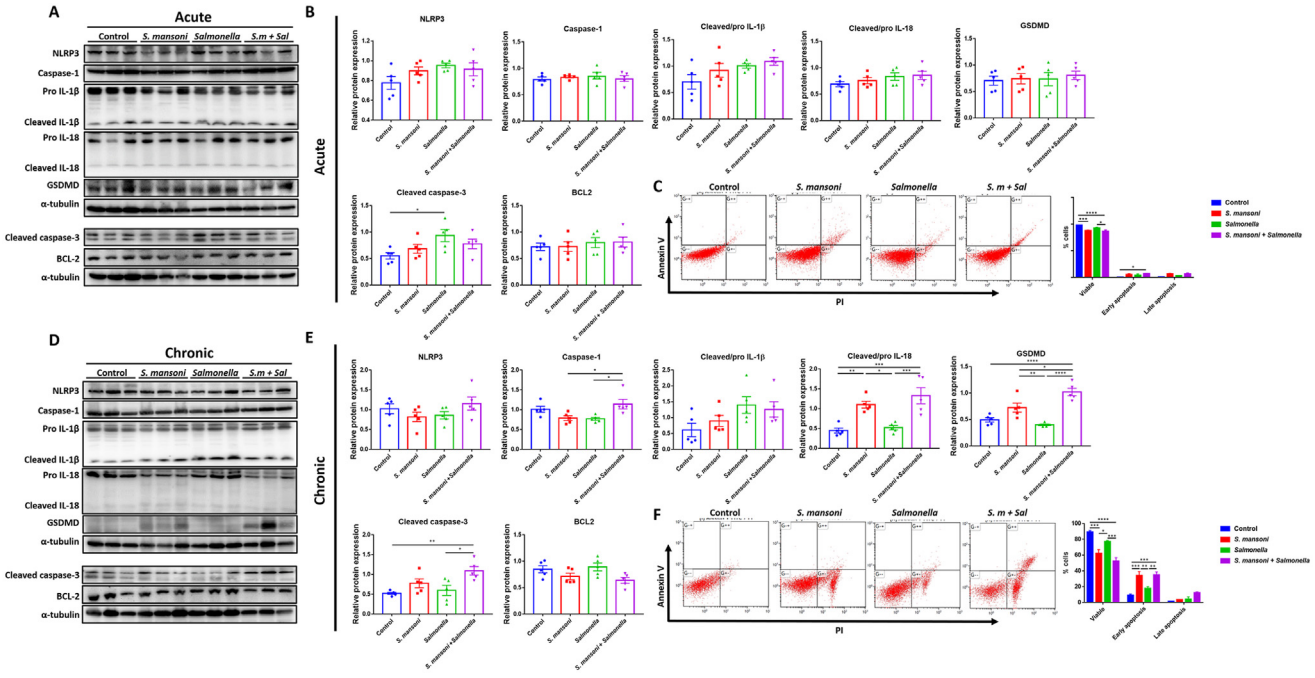

Figure 3. ***S. typhimurium* induces liver inflammasome activation and apoptosis during chronic schistosomiasis.** (A) Representative Western blot images of liver inflammasome and apoptotic markers during acute phase and (B) their relative protein expression levels. No significant differences were observed in the protein level between *S. manosni*-infected mice and co-infected mice during the acute phase. (C) Representative plots showing Annexin V-FITC and PI double staining during acute phase and the percentages of different cell fractions of the total cell population. (D) Representative Western blot images of liver inflammasome and apoptotic markers during chronic phase and (E) their relative protein expression levels. Increased expression of IL-1β, IL-18, GSDMD, and caspase-3 was observed in co-infected mice during the chronic phase. (F) Representative plots showing Annexin V-FITC and PI double staining during chronic phase and the percentages of different cell fractions of the total cell population. Higher number of apoptotic cells was observed in co-infected mice in the chronic phase. All *S. typhimurium* strains used here were TCHST1. Data are shown as mean ± standard error mean (n = 5 per group). *$p < 0.05$; **$p < 0.01$, ***$p < 0.001$, and ****$p < 0.0001$.

Supplementary Fig. 4A, C, and E), and this was accompanied by slightly increased levels of fibrotic markers collagen I and collagen III but not α-SMA (Fig. 4G and I; Supplementary Fig. 4G and I). Unexpectedly, *S. typhimurium* infection at the chronic phase slightly resolved liver fibrosis in *S. mansoni*-infected mice, as indicated by the observed histology (Fig. 4B, D, and F; Supplementary Fig. 4B, D, and F), as well as decreased expression of fibrotic markers (Fig. 4H and J; Supplementary Fig. 4H and J). While similar results can be observed in another experimental trial using the standard *S. typhimurium* strain, ATCC13311 (Supplementary Fig. 4), suggesting that this inhibition of fibrogenesis may not be an incident. The reduction of the number of hepatic eggs in co-infected mice may also provide an explanation for this phenomenon (Fig. 1F; Supplementary Fig. 1F).

S. typhimurium exacerbates splenic injuries but resolves splenic fibrosis

As different bacterial colonization was also observed in the spleen of co-infected mice (Fig. 1B and E; Supplementary Fig. 1B and E), we next investigated whether *S. typhimurium* infection would result in the change of splenic pathology in *S. mansoni*-infected mice. Although splenic weight was not altered (Fig. 5A; Supplementary Fig. 5A), infection of *S. typhimurium* to *S. mansoni*-infected mice resulted in a worsened splenic histology in acute phases (Fig. 5B and C; Supplementary Fig. 5B and C). Protein expression of inflammasome components and apoptotic markers were also consistent with the pathology, as their expression markedly increased in co-infected mice compared with control or mono-infected mice (Fig. 6A and B; Supplementary Fig. 6A). In addition, the number of apoptotic cells in the spleen was much higher in co-infected mice (Fig. 6C). Similarly, *S. typhimurium* infection during chronic schistosomiasis also resulted in a worsened pathology (Fig. 5D—F; Supplementary Fig. 5D—F), as well as an increased expression of inflammasome and apoptotic markers (Fig. 6D—F; Supplementary Fig. 6B). Unexpectedly, *S. typhimurium* infection altered the fibrotic changes in the spleen of *S. mansoni*-infected mice at both acute and chronic phases, as evidenced by a decrease in positive Sirius-red staining (Fig. 7A—D; Supplementary Fig. 7A—D) and decreased collagen I and collagen III expressions (Fig. 7E—H; Supplementary Fig. 7E—H), compared with *S. mansoni*-infected mice. These data suggest that *S. typhimurium* infection differently alters the pathology of the spleen in *S. mansoni*-infected mice by enhancing splenic inflammation and apoptosis, but reducing collagen deposition and fibrosis.

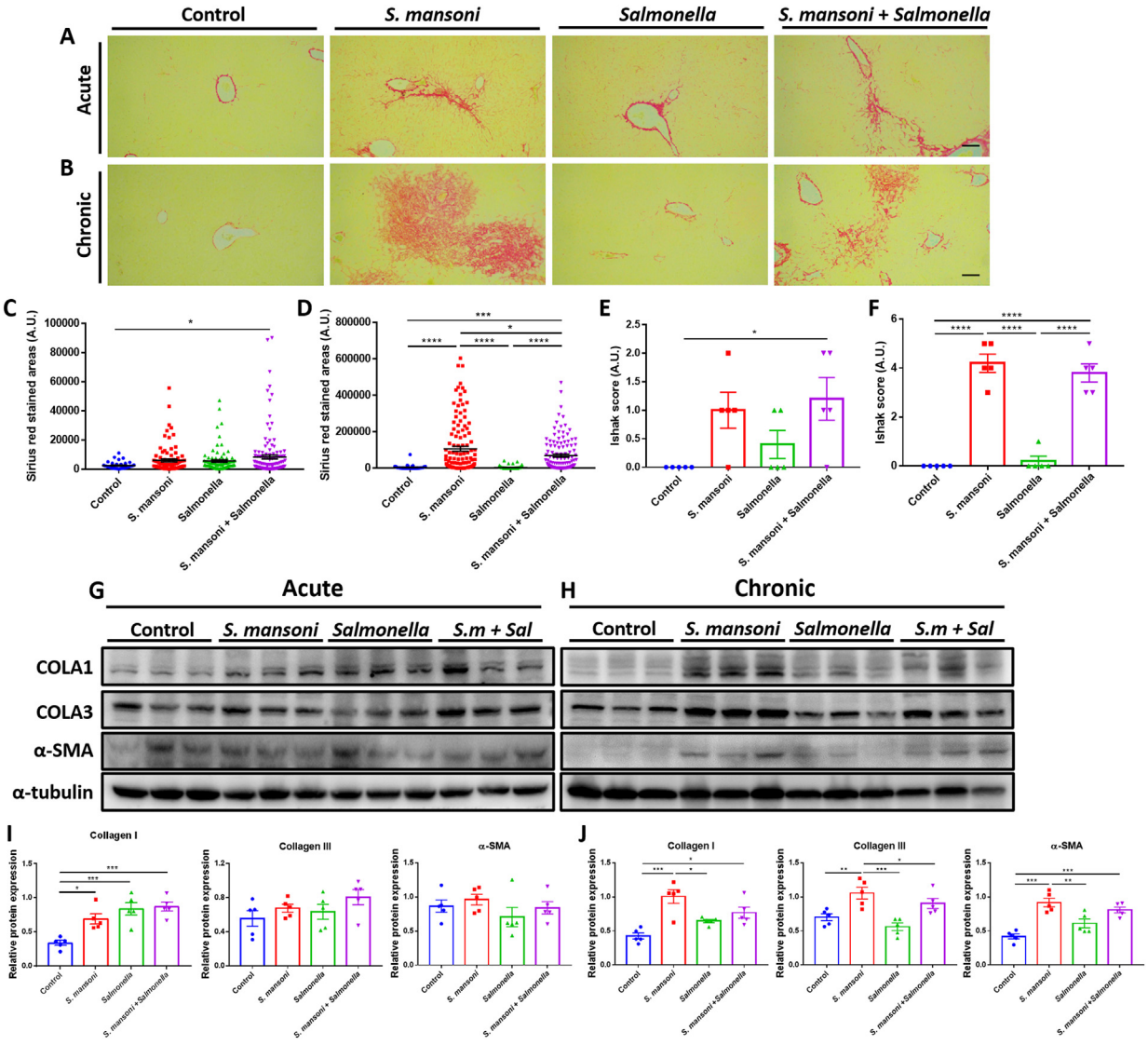

Figure 4. ***S. typhimurium*** **decreased collagen deposition and liver fibrosis during chronic schistosomiasis.** (A—B) Representative Sirius red-stained histological image of the liver during (A) acute phase and (B) chronic phase. Images are shown as 100×magnification and scale bars correspond to 200 μm. (C—D) Quantification of Sirius-red stained areas during (C) acute phase and (D) chronic phase. No significant difference was observed regarding the collagen deposits in the liver between *S. mansoni*-infected mice and co-infected mice during the acute phase; while the livers of co-infected mice showed significantly lower deposition of collagen, fibrous expansion, and bridging compared with *S. mansoni*-infected mice during the chronic phase. Ishak scores of the Sirius-red stained sections during (E) acute phase and (F) chronic phase. (G—H) Representative Western blot images of liver fibrotic markers during (G) acute phase and (H) chronic phase. (I—J) The relative expression level of the protein in (I) acute phase and (J) chronic phase. A slight increase in collagen level was seen in co-infected mice during the acute phase; these levels decreased in co-infected mice during the chronic phase, compared to *S. manosni*-infected mice. All *S. typhimurium* strains used here were TCHST1. Data are shown as mean ± standard error mean (n = 5 per group). $^{*}p < 0.05$; $^{**}p < 0.01$, $^{***}p < 0.001$, and $^{****}p < 0.0001$.

S. typhimurium alters localized immune response of *S. mansoni*-infected mice

To determine the mechanism by which *S. typhimurium* infection alters the existing *S. mansoni*-induced injuries, we measured both cytokine levels and expression in the liver and spleen, as previous studies indicated that immunological changes largely affect the pathology of schistosomiasis.[2] We first confirmed that *S. mansoni* infection induced a downregulated Th2 profile (IL-4, IL-5, and IL-10) and an upregulated Th1 response (IFN-γ and IL-2) in livers of mice from the acute phase; while an upregulated Th2 and downregulated Th1 responses (except for IFN-γ; Fig. 8I) were observed in livers of mice from the chronic phase (Fig. 8 and Supplementary Fig. 8). These results were consistent with previous studies.[2] Livers from co-infected mice at the acute phase showed further depression of a Th2 cytokine, IL-5 and a Th1 cytokine, IL-2 (Fig. 8B and E; Supplementary Fig. 8B and E); and only IFN-γ showed an increased trend in co-infected mice (Fig. 8D). While in the

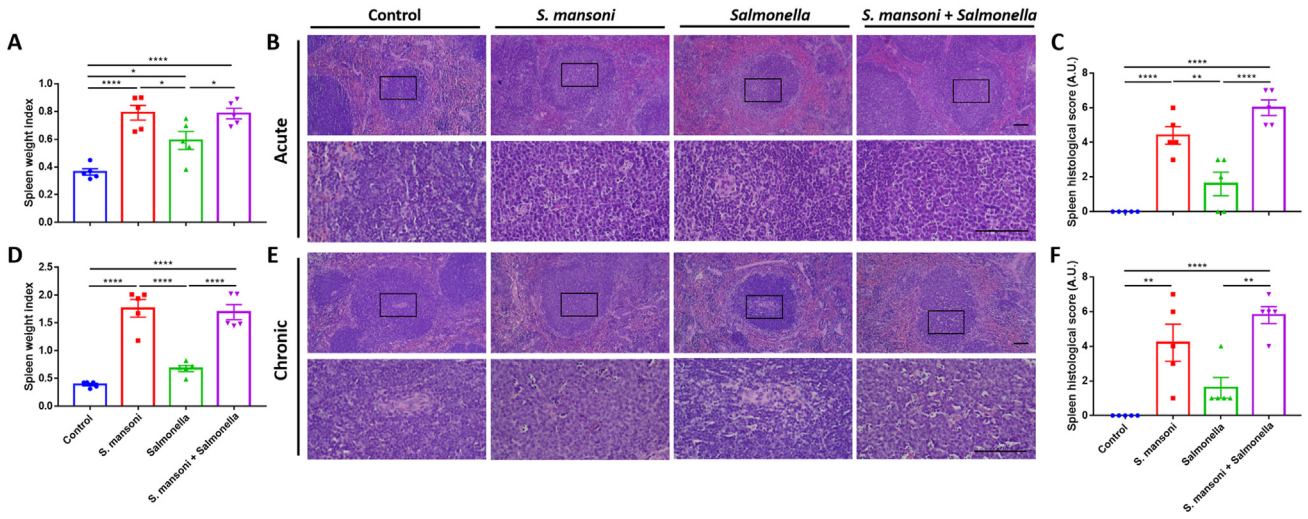

Figure 5. ***S. typhimurium* exacerbates splenic injuries in both acute and chronic schistosomiasis.** (A) Splenic weight index in the acute phase. (B) Representative H&E-stained histological image of the spleen during the acute phase. Both *S. mansoni*-infected mice and co-infected mice showed splenic cell apoptosis (C) Histological scores of the spleen during the acute phase. (D) Splenic weight index in chronic phase. (E) Representative H&E-stained histological image of the spleen during the chronic phase. (F) Histological scores of the spleen during the chronic phase. Images are shown as 100× and 400× magnification and scale bars correspond to 200 μm. All *S. typhimurium* strains used here were TCHST1. Data are shown as mean ± standard error mean (n = 5 per group). *$p < 0.05$; **$p < 0.01$, and ****$p < 0.0001$.

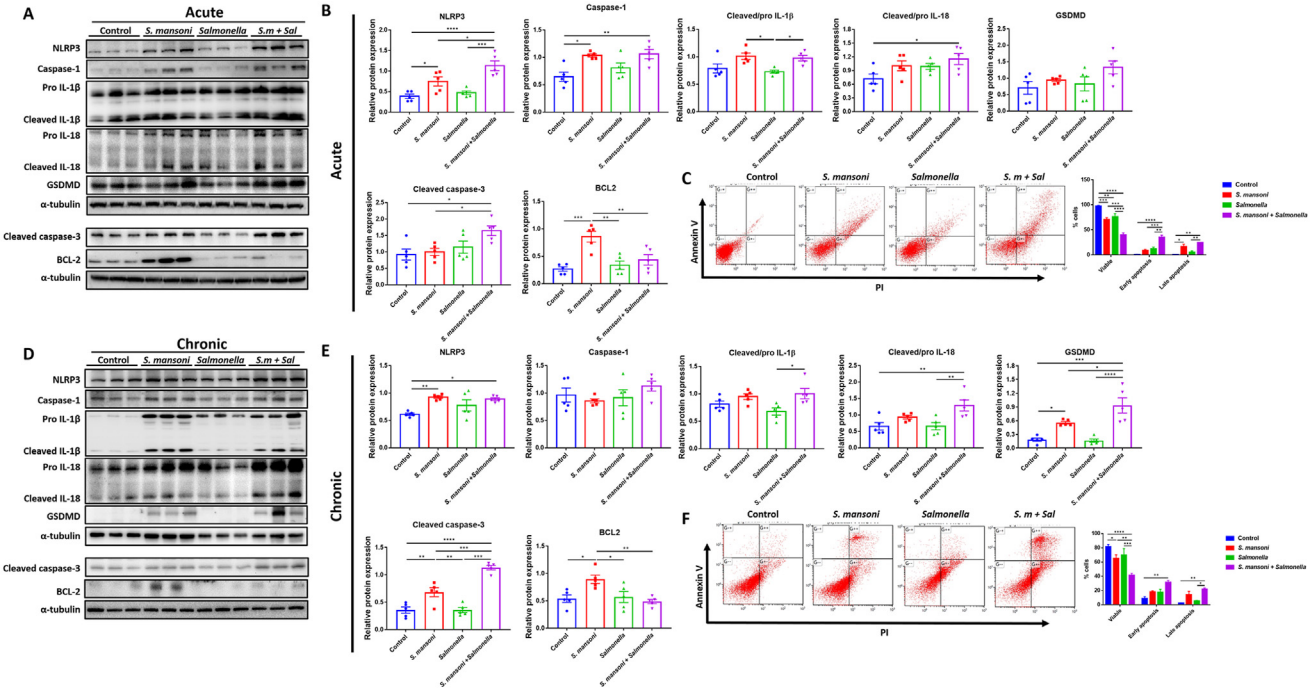

Figure 6. ***S. typhimurium* exacerbates splenic inflammasome activation and apoptosis in both acute and chronic schistosomiasis.** (A) Representative Western blot images of splenic inflammasome and apoptotic markers during acute phase and (B) their relative protein expression levels. (C) Representative plots showing Annexin V-FITC and PI double staining during acute phase and the percentages of different cell fractions of the total cell population. (D) Representative Western blot images of splenic inflammasome and apoptotic markers during chronic phase and their relative protein expression levels. Co-infected mice showed higher expression of GSDMD, and caspase-3 compared to *S. mansoni*-infected mice. (F) Representative plots showing Annexin V-FITC and PI double staining during chronic phase and the percentages of different cell fractions of the total cell population. Higher number of apoptotic cells was observed in co-infected mice in the chronic phase. All *S. typhimurium* strains used here were TCHST1. Data are shown as mean ± standard error mean (n = 5 per group). *$p < 0.05$; **$p < 0.01$, ***$p < 0.001$, and ****$p < 0.0001$.

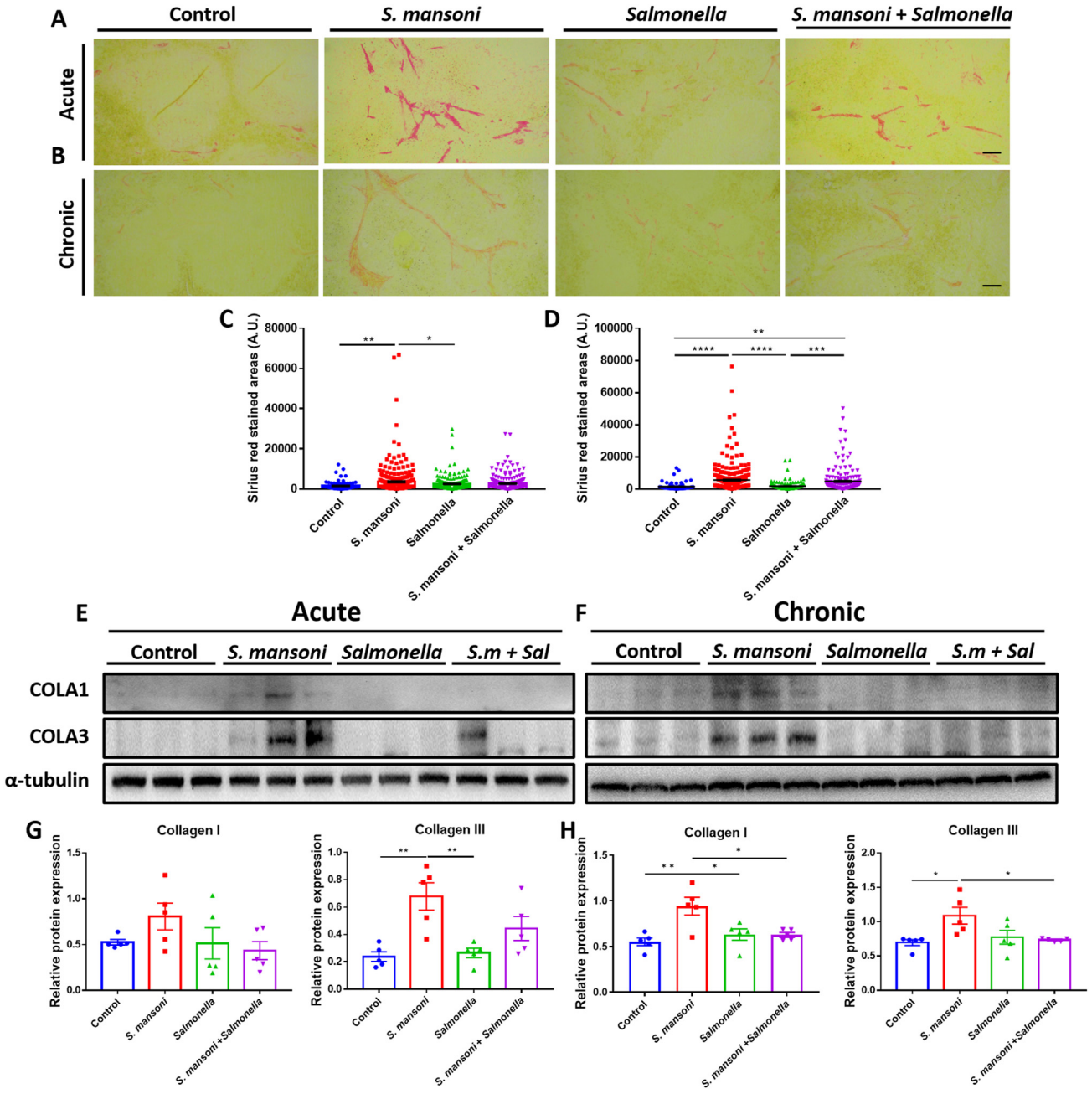

Figure 7. ***S. typhimurium*** **resolves splenic fibrosis in both acute and chronic schistosomiasis.** (A—B) Representative Sirius red-stained histological image of the spleen during (A) acute phase and (B) chronic phase. Images are shown as 100× magnification and scale bars correspond to 200 μm. (C—D) Quantification of Sirius-red stained areas during (C) acute phase and (D) chronic phase. Lower collagen deposits, as well as fibrous bridging, were observed in the spleen of co-infected mice, compared to *S. manosni*-infected mice (E—F) Representative Western blot images of splenic fibrotic markers during (E) acute phase and (F) chronic phase. (G—H) The relative expression level of the protein in (G) acute phase and (H) chronic phase. A decrease in collagen level was seen in co-infected mice compared to *S. manosni*-infected mice. All *S. typhimurium* used here was TCHST1. Data are shown as mean ± standard error mean (n = 5 per group). *$p < 0.05$; ***$p < 0.001$, and ****$p < 0.0001$.

chronic phase, livers from co-infected mice demonstrated a more polarized Th1 response, as indicated by decreased IL-4 and IL-5 levels (Fig. 8F and G; Supplementary Fig. 8F and G) and increased IFN-γ and IL-2 levels (Fig. 8I and J; Supplementary Fig. 8I and J). IL-10, a Th2 cytokine that has also been categorized as a regulatory cytokine,[29,30] also increased in concentration in the liver of co-infected mice (Fig. 8H; Supplementary Fig. 8H).

S. mansoni infection induced a similar immunological response in the spleen, except for a decrease of Th1 cytokines in the acute phase and increased IL-2 concentrations in the chronic phase (Fig. 8; Supplementary Fig. 8).

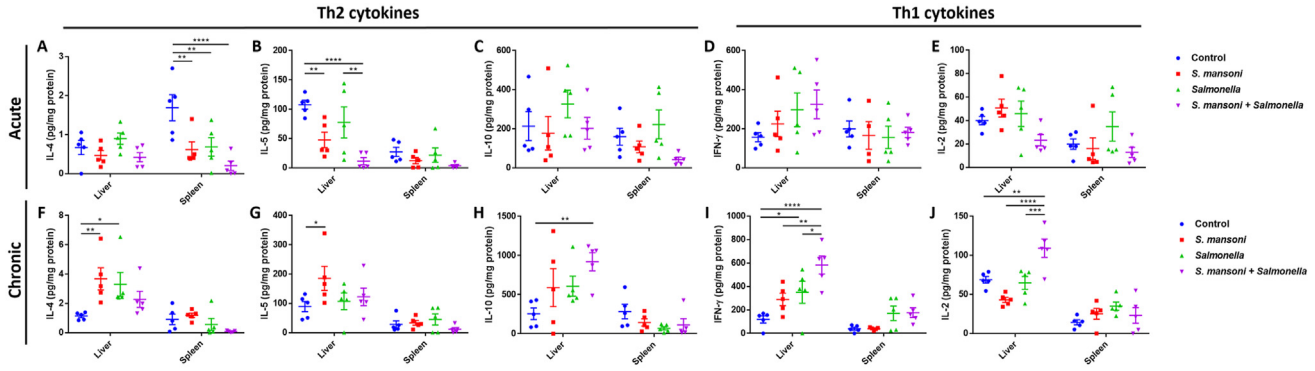

Figure 8. ***S. typhimurium* altered the hepatic and splenic immune response of *S. mansoni*-infected mice.** (A–E) Localized concentration of the cytokine including (A) IL-4, (B) IL-5, (C) IL-10, (D) IFN-γ, and (E) IL-2 in the liver and spleen during the acute phase. (F–J) Localized concentration of the cytokine including (F) IL-4, (G) IL-5, (H) IL-10, (I) IFN-γ, and (J) IL-2 in the liver and spleen during the acute phase. All *S. typhimurium* used here was TCHST1. Data are shown as mean ± standard error mean (n = 5 per group). *$p < 0.05$; **$p < 0.01$, ***$p < 0.001$, and ****$p < 0.0001$.

Co-infected mice at both acute and chronic phases resulted in a depressed splenic Th2 response compared with *S. mansoni*-infected mice (Fig. 8A–C and F–H). With regard to Th1 cytokines, no significant changes were observed in the acute phase (Fig. 8D and E; Supplementary Fig. 8D and E); while increased IFN-γ levels were observed in the chronic phase (Fig. 8I; Supplementary Fig. 8I). Collectively, our findings highlight that *S. typhimurium* infection altered the immune response of *S. mansoni*-infected mice at different timepoint and in different organs, thereby leading to distinct changes in organ pathology.

S. typhimurium altered liver- and splenic-infiltrating immune cells of *S. mansoni*-infected mice

To explore whether the immune cell population might be affected by *S. typhimurium*, we performed immunohistochemistry staining to compare levels of macrophages, CD4+ T cells, and CD8+ T cells between livers and spleens from co-infected mice and mono-infected mice. The results showed that *S. typhimurium* infection resulted in an increase of hepatic macrophages and a slight decrease of CD4+ and CD8+ T cells during acute schistosomiasis (Fig. 9A; Supplementary Fig. 9); while resulting in an increase of CD4+ T cells and a decrease of CD4+ T cells (Fig. 9B; Supplementary Fig. 9). However, *S. typhimurium* infection altered the immune cells population of the spleen neither in acute schistosomiasis nor chronic schistosomiasis (Fig. 9C–D; Supplementary Fig. 9).

Discussion

Although there has been only limited research on the interplay between *Salmonella* infection and schistosomiasis, evidence suggests that this interaction requires more attention.[15–17,19,20] While increased inflammation and apoptosis are expected to happen during co-infection, the decrease in organ fibrosis is unexpected (Figs. 4 and 7; Supplementary Figs. 4 and 7). Though studies have implicated a pro-fibrotic role of *Salmonella* in the intestine,[31,32] the resolution of hepatic or splenic fibrosis with *Salmonella* in schistosomiasis or any other disease has not been reported elsewhere. It is plausible that the altered immunological profiles in co-infected mice sensitize the organs' inflammatory and apoptotic reactions while suppressing the fibrotic responses.[33,34]

In accordance with previous reports, a polarized Th1 response was observed in both the liver and spleen acutely infected with *S. mansoni*, which shifted to a Th2 response during the chronic phase[2]; where that *Salmonella* infection induces a strong and polarized Th1 response.[35,36] Co-infection of *S. mansoni* with *S. typhimurium*, nevertheless, depressed the Th2 response during the acute phase. The decrease of Th2 response seems only intelligible to the decrease of splenic fibrosis but not hepatic fibrosis.[6] Interestingly, the decreased liver Th2 response did not result in the amelioration of liver fibrosis, although the effect was only minimal during co-infection. Their Th1 response also altered differently (increased IFN-γ and decreased IL-2). While collagen expression and their deposition were found to be more severe in co-infected mice, the decrease of IL-4, IL-5, and IL-2 may explain why co-infected livers showed almost unchanged levels of injuries compared with those infected with *S. mansoni* alone.[5,37,38] The decrease of these cytokines may be due to the decreased contribution of CD4+ and CD8+ T cells. While IFN-γ promotes macrophage activation and antibacterial immunity,[39] its increase during co-infection may explain the increased hepatic macrophages and decrease in tissue bacterial counts.

During the chronic phase, co-infected livers and spleens showed a decreased IL-4 and IL-5 profiles and an increased IL-10, IFN-γ, and IL-2 compared to mono-infected livers. This cytokine profile suggested that the local immunity shifted back from a pro-fibrogenic Th2 to an anti-fibrotic Th1 response, which therefore contributes to the resolution of liver and splenic fibrosis.[2,7] However, both hepatic and splenic injuries were further exacerbated during co-infection, which could be caused by the increase of localized *S. typhimurium*. This finding is similar to those

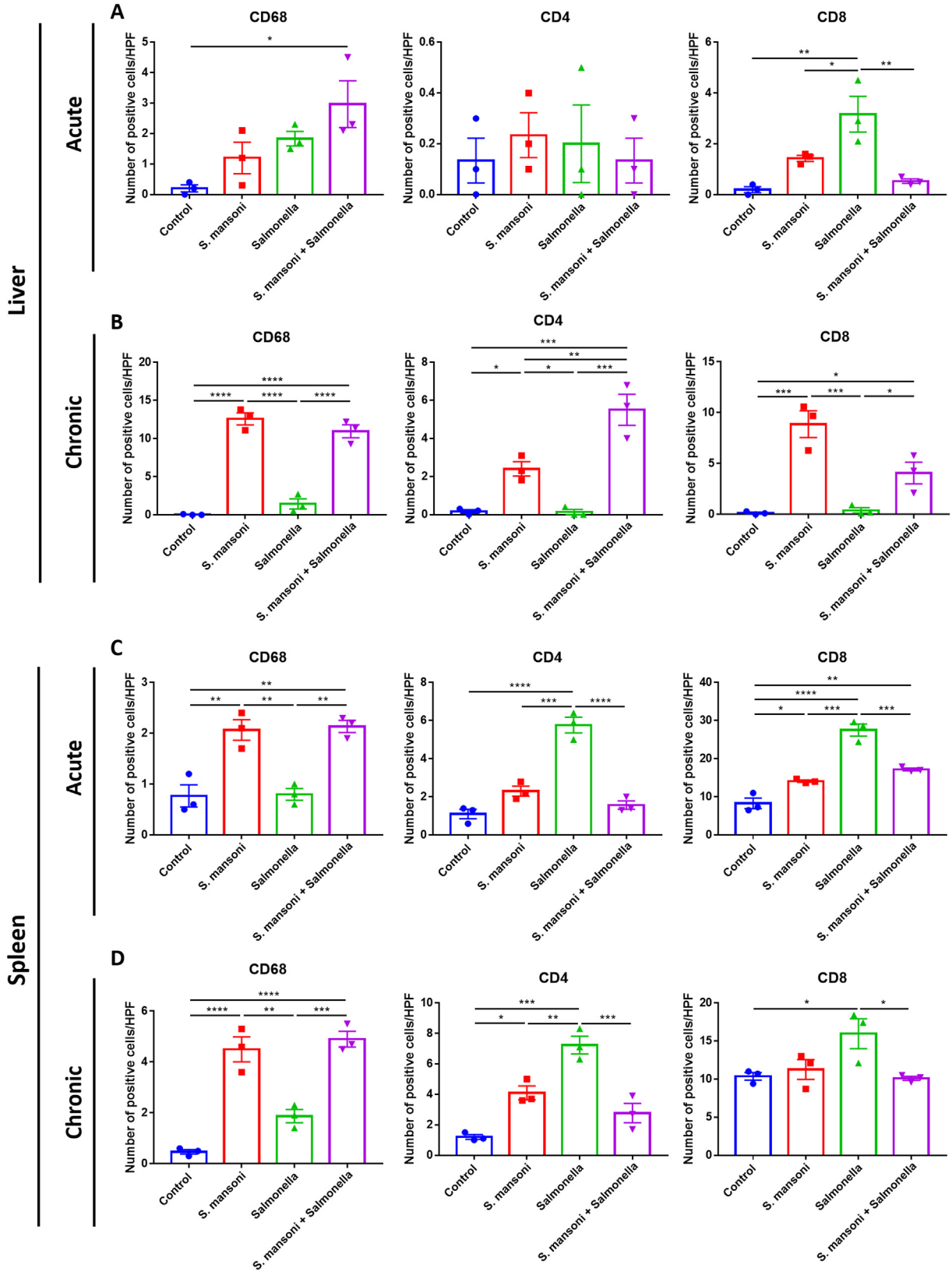

Figure 9. ***S. typhimurium*** **altered liver-infiltrating immune cells of** ***S. mansoni*****-infected mice.** The number of CD68, CD4, and CD8 immuno-positive cells per high power field (HPF) observed in the liver of mice during (A) acute phase and (B) chronic phase. *S. typhimurium* infection altered the infiltration of these immune cells in the liver of *S. mansoni*-infected mice. The number of immuno-positive cells per HPF observed in the spleen of mice during (C) acute or (D) chronic schistosomiasis. No changes were observed in co-infected mice, compared to *S. mansoni*-infected mice. Representative immunohistochemistry staining of the slides were shown in Supplementary Fig. 9. All *S. typhimurium* strain used here was TCHST1. Data are shown as mean ± standard error mean (n = 3 per group). *$p < 0.05$; **$p < 0.01$, ***$p < 0.001$, and ****$p < 0.0001$.

previously reported.[15,17,21] Although hepatic IFN-γ also increased, the number of macrophages was not changed compared to *S. mansoni*-infected livers. In addition, a reduction of hepatic CD8+ T cells and increased CD4+ T cells may suggest local immunodeficiency which fails to clear pathogens. Similar to the acute phase, the number of splenic infiltrating cells in co-infected mice did not change compared to *S. mansoni*-infected mice. IL-10, unlike other Th1 or Th2 cytokines which show distinct function, are highly scenario-dependent. Therefore, IL-10 can play roles in both inflammatory and anti-inflammatory situations.[40–43] Since fibrosis is usually the endpoint of inflammation,[44] the alternation of inflammation may mediate the fibrotic process.[45] Several reports have also suggested that IL-10 can through its anti-inflammatory role to inhibit fibrosis.[29,30,46,47] However, in this study, the resolution of fibrosis did not accompany a decreased inflammation. A critical question raised by our findings is whether IL-10 takes place in regulating the immunity during co-infection of *S. mansoni* and *S. typhimurium*, and further studies may be needed to establish their mechanism in this situation. Aside from that, the decreased entrapment of liver eggs may also directly lead to decreased fibrogenesis.

Lastly, *S. typhimurium* is more likely to colonize the organs during the chronic phase of schistosomiasis than in the acute phase. This may thereby lead to a lesser secretion of *S. typhimurium* in the stool. While it is possible to observe an undetectable number of schistosome eggs at the acute phase because at that time the adult worms are still finding their way to the mesenteric circulation, the number of tissue eggs was found to be decreased in co-infected mice in the chronic phase (Fig. 1; Supplementary Fig. 1). Previous reports have suggested that *S. typhimurium* can bind to the schistosome tegument by their surface fimbriae or pili[48,49]; thereby affecting egg production of *S. mansoni* and relieving egg-induced fibrosis.[22] In addition, *S. typhimurium* may colonize the *S. mansoni*-induced lesions leading to a higher bacterial burden.[50] On top of that, *S. typhimurium* infection may lower the blood-sucking activities of *S. mansoni* as indicated by improvement of different red blood cell (RBC) indices in the mice's peripheral blood (Supplementary Fig. 10), suggesting that *S. typhimurium* indeed interacts with *S. mansoni* worms; and this is therefore a fundamental issue for further research.

Collectively, our findings here demonstrated that *S. mansoni*-infected mice challenged with *S. typhimurium* had higher bacterial colonization in the chronic phase. Infection with *S. typhimurium* during chronic schistosomiasis led to more drastic damage but unexpectedly lower fibrotic deposits in the liver and spleen. Further, co-infection alters the immunological functioning of the mice, possibly the reason for the observed pathological outcomes.

Declaration of competing interest

All authors declare that they have no conflict of interest.

Acknowledgments

We thank National Laboratory Animal Center (NLAC), NARLabs, Taiwan, for technical support in biochemistry analysis. This work was supported in part by grants from the Ministry of Science and technology of Taiwan (Grant number: MOST-110-2320-B-320-004) and Tzu Chi Foundation, Taiwan (Grant number: TCU-B01). The funders had no role in study design, data collection and interpretation, or the decision to submit the work for publication.

References

1. McManus DP, Dunne DW, Sacko M, Utzinger J, Vennervald BJ, Zhou X-N. Schistosomiasis. *Nat Rev Dis Prim* 2018;**4**:13.
2. Wilson MS, Mentink-Kane MM, Pesce JT, Ramalingam TR, Thompson R, Wynn TA. Immunopathology of schistosomiasis. *Immunol Cell Biol* 2007;**85**:148–54.
3. Mansfield JM, Cêtre C, Pierrot C, Cocude C, Lafitte S, Capron A, et al. Profiles of Th1 and Th2 cytokines after primary and secondary infection by Schistosoma mansoni in the semi-permissive rat host. *Infect Immun* 1999;**67**:2713–9.
4. Coutinho HM, Acosta LP, Wu HW, McGarvey ST, Su L, Langdon GC, et al. Th2 cytokines are associated with persistent hepatic fibrosis in human Schistosoma japonicum infection. *J Infect Dis* 2007;**195**:288–95.
5. de Jesus AR, Magalhães A, Miranda DG, Miranda RG, Araújo MI, de Jesus AA, et al. Association of type 2 cytokines with hepatic fibrosis in human Schistosoma mansoni infection. *Infect Immun* 2004;**72**:3391–7.
6. Barron L, Wynn TA. Fibrosis is regulated by Th2 and Th17 responses and by dynamic interactions between fibroblasts and macrophages. *Am J Physiol Gastrointest Liver Physiol* 2011; **300**:G723–8.
7. Gieseck RL, Wilson MS, Wynn TA. Type 2 immunity in tissue repair and fibrosis. *Nat Rev Immunol* 2018;**18**:62–76.
8. Muok EM, Mwinzi PN, Black CL, Carter JM, Ng'ang'a ZW, Gicheru MM, et al. Short report: childhood coinfections with Plasmodium falciparum and Schistosoma mansoni result in lower percentages of activated T cells and T regulatory memory cells than schistosomiasis only. *Am J Trop Med Hyg* 2009; **80**:475–8.
9. Legesse M, Erko B, Balcha F. Increased parasitaemia and delayed parasite clearance in Schistosoma mansoni and Plasmodium berghei co-infected mice. *Acta Trop* 2004;**91**:161–6.
10. Abou Holw SA, Anwar MM, Bassiouni RB, Hussen NA, Eltaweel HA. Impact of coinfection with Schistosoma mansoni on Helicobacter pylori induced disease. *J Egypt Soc Parasitol* 2008;**38**:73–84.
11. Bhattacharjee S, Mejías-Luque R, Loffredo-Verde E, Toska A, Flossdorf M, Gerhard M, et al. Concomitant infection of S. mansoni and H. pylori promotes promiscuity of antigen-experienced cells and primes the liver for a lower fibrotic response. *Cell Rep* 2019;**28**:231–244.e5.
12. Carvalho EM, Andrews BS, Martinelli R, Dutra M, Rocha H. Circulating immune complexes and rheumatoid factor in schistosomiasis and visceral leishmaniasis. *Am J Trop Med Hyg* 1983;**32**:61–8.
13. Igwe NN, Agbo EB, editors. *Incidence of co-infection of enteric Salmonella and Schistosoma in Kachia local government area of Kaduna state, Nigeria*; 2014.

14. Mohager MO, Mohager SO, Kaddam LA, JIJoPS, Research. *The association between shistosomiasis and enteric fever in a single Schistosoma endemic area in Sudan*. 5. 2014. p. 2181.
15. Mbuyi-Kalonji L, Barbé B, Nkoji G, Madinga J, Roucher C, Linsuke S, et al. Non-typhoidal Salmonella intestinal carriage in a Schistosoma mansoni endemic community in a rural area of the Democratic Republic of Congo. *PLoS Neglected Trop Dis* 2020;**14**:e0007875.
16. Marege A, Seid M, Boke B, Thomas S, Arage M, Mouze N, et al. Prevalence of Schistosoma mansoni-Salmonella coinfection among patients in southern Ethiopia. *New Microbes New Infect* 2021;**40**:100842.
17. Rocha H, Kirk JW, Hearey Jr CD. Prolonged Salmonella bacteremia in patients with Schistosoma mansoni infection. *Arch Intern Med* 1971;**128**:254—7.
18. Lambertucci JR, Godoy P, Neves J, Bambirra EA, Ferreira MD. Glomerulonephritis in Salmonella-Schistosoma mansoni association. *Am J Trop Med Hyg* 1988;**38**:97—102.
19. Njunda AL, Oyerinde JP. Salmonella typhi infection in Schistosoma mansoni infected mice. *West Afr J Med* 1996;**15**:24—30.
20. Tuazon CU, Nash T, Cheever A, Neva F, Lininger L. Influence of salmonella bacteremia on the survival of mice infected with Schistosoma mansoni. *J Infect Dis* 1985;**151**:1166—7.
21. Collins FM, Boros DL, Warren KS. The effect of Schistosoma mansoni infection on the response of mice to Salmonella enteritidis and Listeria monocytogenes. *J Infect Dis* 1972;**125**:249—56.
22. Zhu X, Chen L, Wu J, Tang H, Wang Y. Salmonella typhimurium infection reduces schistosoma japonicum worm burden in mice. *Sci Rep* 2017;**7**:1349.
23. Lam HYP, Liang T-R, Peng S-Y. Ameliorative effects of Schisandrin B on Schistosoma mansoni-induced hepatic fibrosis in vivo. *PLoS Neglected Trop Dis* 2021;**15**:e0009554.
24. Bärenbold O, Raso G, Coulibaly JT, N'Goran EK, Utzinger J, Vounatsou P. Estimating sensitivity of the Kato-Katz technique for the diagnosis of Schistosoma mansoni and hookworm in relation to infection intensity. *PLoS Neglected Trop Dis* 2017;**11**:e0005953.
25. Cheever AW. Conditions affecting the accuracy of potassium hydroxide digestion techniques for counting Schistosoma mansoni eggs in tissues. *Bull World Health Organ* 1968;**39**:328—31.
26. Veteläinen RL, Bennink RJ, de Bruin K, van Vliet A, van Gulik TM. Hepatobiliary function assessed by 99mTc-mebrofenin cholescintigraphy in the evaluation of severity of steatosis in a rat model. *Eur J Nucl Med Mol Imag* 2006;**33**:1107—14.
27. Nallagangula KS, Nagaraj SK, Venkataswamy L, Chandrappa M. Liver fibrosis: a compilation on the biomarkers status and their significance during disease progression. *Fut Sci OA* 2018;**4**:Fso250.
28. Dkhil MA, Al-Quraishy S, Al-Khalifa MS. The effect of Babesia divergens infection on the spleen of Mongolian gerbils. *BioMed Res Int* 2014;**2014**:483854.
29. Mosser DM, Zhang X. Interleukin-10: new perspectives on an old cytokine. *Immunol Rev* 2008;**226**:205—18.
30. Couper KN, Blount DG, Riley EM. *IL-10: the master regulator of immunity to infection*. 180. 2008. p. 5771—7.
31. Ehrhardt K, Steck N, Kappelhoff R, Stein S, Rieder F, Gordon IO, et al. Persistent Salmonella enterica serovar typhimurium infection induces protease expression during intestinal fibrosis. *Inflamm Bowel Dis* 2019;**25**:1629—43.
32. Grassl GA, Valdez Y, Bergstrom KSB, Vallance BA, Finlay BB. Chronic enteric Salmonella infection in mice leads to severe and persistent intestinal fibrosis. *Gastroenterology* 2008;**134**:768—80. .e2.
33. Arango Duque G, Descoteaux A. *Macrophage cytokines: involvement in immunity and infectious diseases*. 2014. 5.
34. Seow HF. Pathogen interactions with cytokines and host defence: an overview. *Vet Immunol Immunopathol* 1998;**63**:139—48.
35. O'Donnell H, Mcsorley S. *Salmonella as a model for non-cognate Th1 cell stimulation*. 2014. 5.
36. Mizuno Y, Takada H, Nomura A, Jin CH, Hattori H, Ihara K, et al. Th1 and Th1-inducing cytokines in Salmonella infection. *Clin Exp Immunol* 2003;**131**:111—7.
37. León B, Ballesteros-Tato A. *Modulating Th2 cell immunity for the treatment of asthma*. 2021. 12.
38. Tsoutsou PG, Gourgoulianis KI, Petinaki E, Germenis A, Tsoutsou AG, Mpaka M, et al. Cytokine levels in the sera of patients with idiopathic pulmonary fibrosis. *Respir Med* 2006;**100**:938—45.
39. Tau G, Rothman P. Biologic functions of the IFN-gamma receptors. *Allergy* 1999;**54**:1233—51.
40. King A, Balaji S, Marsh E, Le LD, Shaaban AF, Crombleholme TM, et al. Interleukin-10 regulates the fetal hyaluronan-rich extracellular matrix via a STAT3-dependent mechanism. *J Surg Res* 2013;**184**:671—7.
41. Louis H, Van Laethem JL, Wu W, Quertinmont E, Degraef C, Van den Berg K, et al. Interleukin-10 controls neutrophilic infiltration, hepatocyte proliferation, and liver fibrosis induced by carbon tetrachloride in mice. *Hepatology* 1998;**28**:1607—15.
42. Louis H, Le Moine O, Goldman M, Devière J. Modulation of liver injury by interleukin-10. *Acta Gastroenterol Belg* 2003;**66**:7—14.
43. Demols A, Van Laethem JL, Quertinmont E, Degraef C, Delhaye M, Geerts A, et al. Endogenous interleukin-10 modulates fibrosis and regeneration in experimental chronic pancreatitis. *Am J Physiol Gastrointest Liver Physiol* 2002;**282**:G1105—12.
44. Wynn TA, Ramalingam TR. Mechanisms of fibrosis: therapeutic translation for fibrotic disease. *Nat Med* 2012;**18**:1028—40.
45. Wynn TA. Cellular and molecular mechanisms of fibrosis. *J Pathol* 2008;**214**:199—210.
46. Ip WKE, Hoshi N, Shouval DS, Snapper S, Medzhitov R. Anti-inflammatory effect of IL-10 mediated by metabolic reprogramming of macrophages. *Science* 2017;**356**:513—9.
47. Steen EH, Wang X, Balaji S, Butte MJ, Bollyky PL, Keswani SG. The role of the anti-inflammatory cytokine interleukin-10 in tissue fibrosis. *Adv Wound Care* 2019;**9**:184—98.
48. Barnhill AE, Novozhilova E, Day TA, Carlson SA. Schistosoma-associated Salmonella resist antibiotics via specific fimbrial attachments to the flatworm. *Parasites Vectors* 2011;**4**:123.
49. Melhem RF, LoVerde PT. Mechanism of interaction of Salmonella and Schistosoma species. *Infect Immun* 1984;**44**:274—81.
50. Ashour DS, Othman AA. Parasite—bacteria interrelationship. *Parasitol Res* 2020;**119**:3145—64.

Appendix A. Supplementary data

Supplementary data to this article can be found online at https://doi.org/10.1016/j.jmii.2023.03.002.